Molecular Vision 2025; 31:584-595 <http://www.molvis.org/molvis/v31/584>
Received 28 September 2025 | Accepted 29 December 2025 | Published 31 December 2025

Reticular fiber distribution in sclera: Key to understanding pathologic myopia and posterior staphylomas

Hirohiko Kakizaki,[1,2] Heebae Ahn,[2] Muhammad Abumanhal,[3] Derrick Lian,[4] Kan Ishijima,[5] Hidenori Mito,[6] Naoyuki Morishige[7]

[1]Asami Eye Surgery Clinic. Obu, Aichi, Japan; [2]Department of Ophthalmology, College of Medicine, Dong-A University. Saha, Busan, Korea; [3]Oculoplastic, Orbital and Lacrimal Institute, Division of Ophthalmology. Tel Aviv Medical Center, Tel Aviv, Israel; [4]Department of Pathology, National University Hospital, Singapore; [5]Sapporo Ophthalmology and Oculoplastic Surgery Clinic, Sapporo, Hokkaido, Japan; [6]Ide Eye Hospital, Yamagata, Japan; [7]Ohshima Eye Hospital, Hakata, Fukuoka, Japan

Purpose: To characterize the distribution of reticular fibers in the human sclera and explore their potential role in the pathogenesis of pathologic myopia and posterior staphyloma.
Methods: Central sagittal sections of 13 globes (6 right eyes and 7 left eyes) were obtained from 12 East Asian cadavers aged 38–94 years (mean age: 74.9 years). Three scleral regions were examined: the pars plana, 3:00–3:30 clock-hour position, and 5:00–5:30 clock-hour position. Specimens were fixed in 10% formalin and stained with silver nitrate. ImageJ software was used for image processing and quantification of fiber density.
Results: Reticular fiber density exhibited considerable inter- and intraindividual variability. The average densities at the pars plana, 3:00–3:30, and 5:00–5:30 were 31.07%, 26.10%, and 22.70%, respectively. Density ranges were 23.46%–58.51% (pars plana), 19.18%–43.07% (3:00–3:30), and 13.48%–50.95% (5:00–5:30). In 10 eyes, the pars plana showed the highest density, followed by 3:00–3:30 and then 5:00–5:30. Two eyes had the lowest density at 3:00–3:30, while one eye exhibited the highest density in this region.
Conclusions: Reticular fiber density in the sclera exhibits considerable interindividual variability. Our findings suggest that regions of structural vulnerability within the sclera may extend beyond the posterior pole, potentially offering new insights into the pathogenesis of posterior staphyloma. A reduction in reticular fiber density may be implicated in the progression of pathologic myopia and the development of posterior staphylomas, although further investigation is warranted to substantiate this association.

Reticular fibers are one of the three major components of the extracellular fibrous matrix in the human body. Unlike collagen and elastic fibers [1], reticular fibers have been poorly studied and have received limited attention in the field of ophthalmology.

These fibers consist of fine fibrils (<20 µm in diameter) that form extensive networks and structural frameworks in soft tissues [1]. Composed primarily of type III collagen, reticular fibers differ from the more abundant type I collagen fibers [1]. They do not stain with hematoxylin and eosin or Masson's trichrome but are distinctly visualized using silver impregnation techniques [1,2]. Degenerative changes in reticular fibers are commonly observed with aging [3]. Reticular and collagen fibers are continuous with one another, exchanging fibrils to form an integrated network [1].

Despite this continuity, reticular and collagen fibers differ in several structural and functional aspects [1]. Fresh collagen fibers vary widely in thickness (1–100 µm), typically exhibit a wavy and nonbranching appearance, and form bundles of closely packed fibrils [1]. Proteoglycan filaments connect adjacent collagen fibrils, regulate their spacing, and stabilize their bundling, contributing to the tissue-specific organization of collagen [1].

Reticular fibers exhibit variable malleability, allowing them to maintain flexibility under pressure fluctuations [4]. In contrast, collagen fibers possess greater mechanical strength but lower malleability, making them less adaptable to such changes [4].

Pathologic myopia is characterized by abnormal ocular morphology, including excessive axial elongation and the formation of posterior staphylomas [5]. Although several morphologic subtypes of posterior staphyloma have been reported [5–7], only a few histologic studies have investigated its pathogenesis [8–10], and these have focused exclusively on collagen fibers, without examining reticular fibers.

Axial elongation in myopia is associated with remodeling of the scleral connective tissue [11], involving changes in collagen fiber alignment, reduced collagen content, and alterations in extracellular matrix composition, ultimately leading to decreased mechanical stiffness of the sclera [11]. Notably,

Correspondence to: Hirohiko Kakizaki, Asami Eye Surgery Clinic 2-165, Toshinchou, Obu, Aichi 474-1173, Japan, Phone: +81-562-46-7700; FAX: +81-562-46-7707; email: cosme_geka@yahoo.co.jp

reticular fibers transiently increase and are subsequently replaced by collagen fibers during the early inflammatory phase of wound healing [12]. The purpose of the present study was to demonstrate the distribution of reticular fibers in the human sclera to gain insights into the potential pathology of pathologic myopia and posterior staphyloma.

METHODS

Central sagittal sections of 13 globes (6 right, 7 left), including the sclera, were obtained from 12 East Asian cadavers aged 38–94 years (mean age: 74.9 years). Specimens were fixed in 10% formalin for histologic examination.

The procedures for harvesting and preparing the samples were as follows. First, the tissue from the skin to the periosteum was circumferentially incised approximately 5 mm beyond the orbital aperture using a No. 15 surgical blade. A raspatory was used to detach the periosteum, and the periorbita was carefully separated toward the orbital apex. The nerves, blood vessels, and nasolacrimal duct passing through the orbital wall were transected. After removal of the lateral orbital wall to a depth of approximately 3 cm from the orbital rim, the orbital contents were dissected with a No. 11 surgical blade parallel to the coronal plane. The specimens were then sagittally sectioned at the midpoint of the horizontal eyelid fissure to include the central globe, using a sharp razor on a hard plate. Sections were processed, paraffin-embedded, and cut into 6-μm slices for microscopic analysis. Reticular fibers were stained using the Reticulum II Staining Kit on a BenchMark Special Stains instrument (Roche Diagnostics, Pleasanton, CA). This kit is a modified version of Gordon and Sweet's stain [13].

Microscopic images were captured using a digital camera system mounted on a microscope (Swift Microscope World,

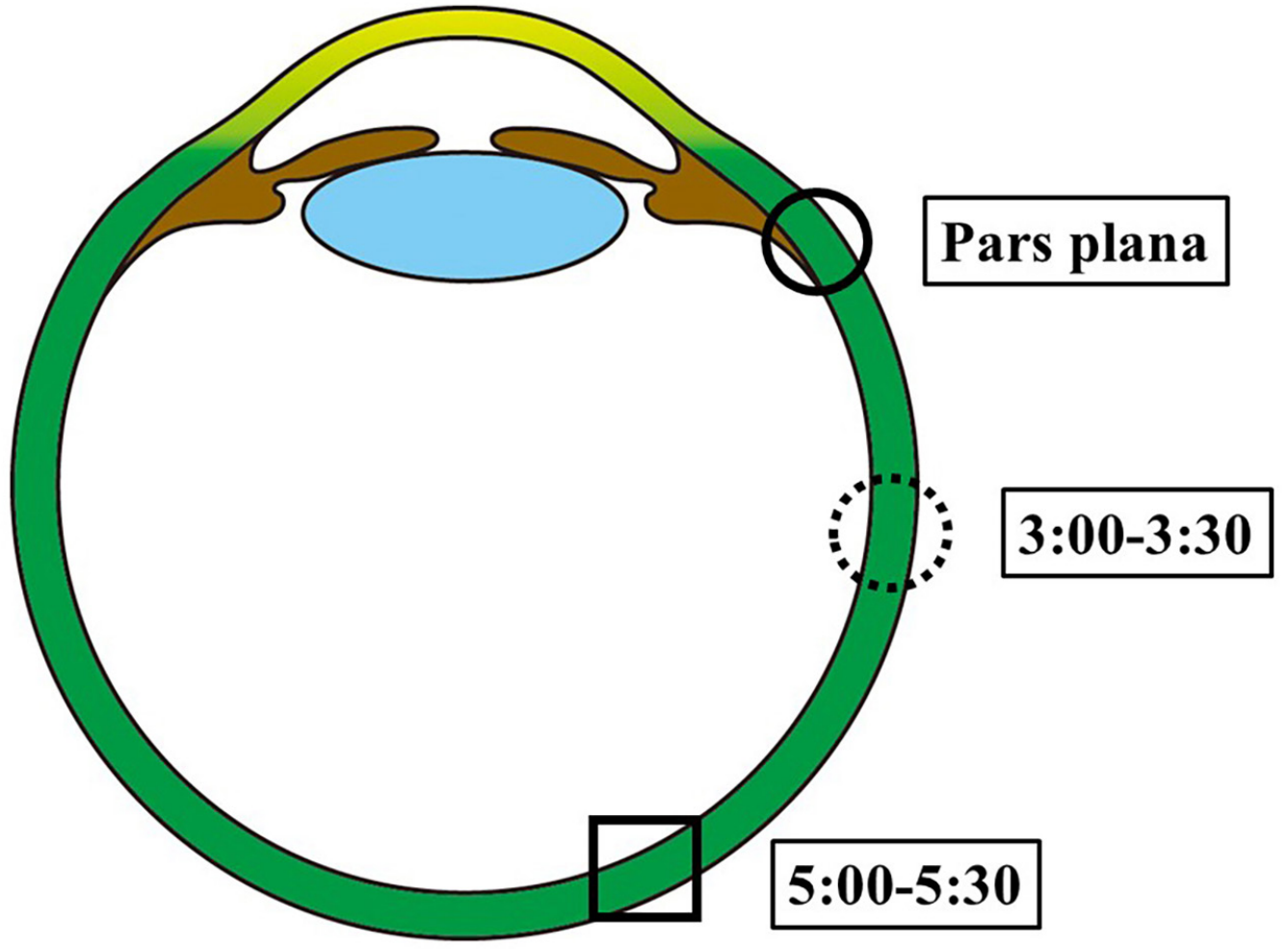

Figure 1. Three regions of the sclera examined in this study: pars plana, 3:00–3:30 clock-hour position, and 5:00–5:30 clock-hour position.

Carlsbad, CA). Because each microphotograph covered only a small area, images were assembled into a single montage to display the entire section using Adobe Photoshop 2024 (Adobe Systems, San Jose, CA).

Three regions of the sclera were examined: the pars plana, 3:00–3:30 clock-hour position, and 5:00–5:30 clock-hour position (Figure 1). Fiji software (ImageJ; National Institutes of Health, Bethesda, MD, USA) was used for image processing and fiber density measurement. The method included color deconvolution to enhance the visualization of stained reticular fibers. All images were standardized using the same color scale and contrast settings, then converted to grayscale (Figure 2A, B). Each image was subsequently binarized (black and white) to enable quantitative analysis (Figure 2C). Reticular fiber density was calculated as the ratio of fiber-positive area to total image area. All image analyses were manually performed by the same observer (Muhammad Abumanhal) using ImageJ, with a consistent thresholding level applied across all images. Therefore, segmentation was uniform throughout the data set, and interobserver validation was not applicable.

Quantitative comparison of reticular fiber density among the three scleral regions was performed using one-way ANOVA. A p value <0.05 was considered statistically significant. When significance was observed, a post hoc test (Bonferroni correction) was conducted to identify specific group differences. To compare reticular fiber density between younger and older individuals, a *t* test was performed using the same software and significance threshold.

Outliers were identified using box-and-whisker plots to visually assess data distribution. Normality was evaluated using the Shapiro-Wilk and Kolmogorov–Smirnov tests. When outliers were detected, analyses were repeated after their exclusion to confirm the robustness of the results. All statistical analyses were conducted using IBM SPSS Statistics for Windows, version 29.0 (IBM Corp., Armonk, NY). This study was approved by the Institutional Review Board of Dong-A University Hospital (approval number: DAUHIRB-EXP-25–114) and was conducted in accordance with the tenets of the Declaration of Helsinki and its later amendments.

RESULTS

The data are summarized in Table 1. Reticular fiber density demonstrated considerable interindividual variability but tended to decrease toward the posterior region. The average densities at the pars plana, 3:00–3:30 clock-hour position, and 5:00–5:30 clock-hour position were 31.07%, 26.10%, and 22.70%, respectively. The corresponding ranges were 23.46%–58.51% (pars plana; median: 29.30%, standard deviation: 9.34%), 19.18%–43.07% (3:00–3:30; median: 25.18%, standard deviation: 6.47%), and 13.48%–50.95% (5:00–5:30; median: 19.77%, standard deviation: 9.18%). Figure 3 presents a box-and-whisker plot illustrating these distributions.

In 10 eyes, the pars plana exhibited the highest density, followed by 3:00–3:30 and then 5:00–5:30 (Figure 4 and Figure 5). Two eyes—a 38-year-old male and an 81-year-old female—showed the lowest density at 3:00–3:30 (Figure 6 and Figure 7), while one eye from a 79-year-old male demonstrated the highest density at this location (Figure 8 and Figure 9).

Outliers were identified in case 12: one in the pars plana (58.51%), one in the 3:00–3:30 region (43.07%), and one in the 5:00–5:30 region (50.95%; Figure 3). These values were

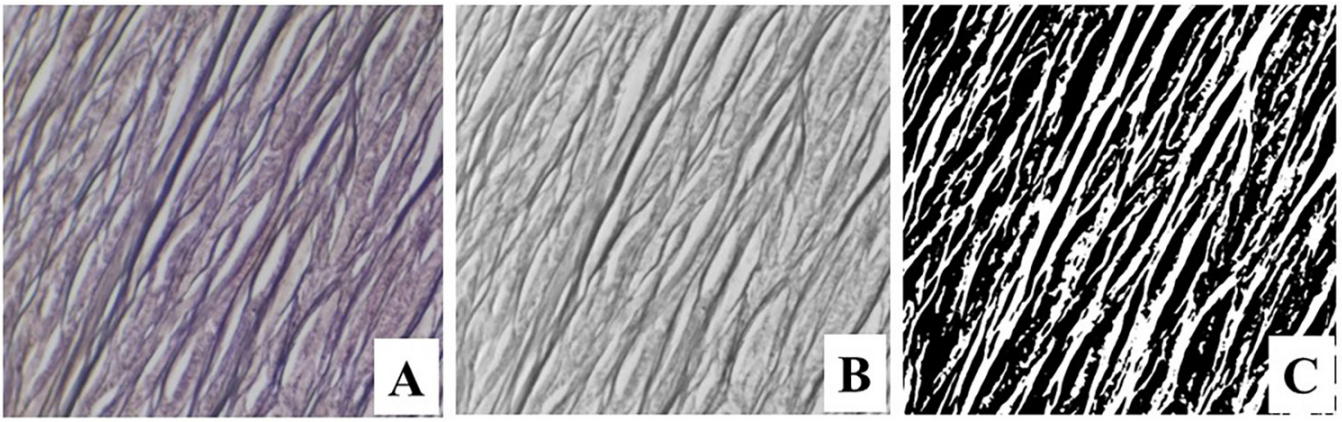

Figure 2. Image processing workflow. **A**: Original stained image is illustrated. **B**: Reticular fibers are outlined. **C**: Final binary (white and black) image is used for analysis. White areas indicate reticular fibers.

Table 1. Reticular fiber density in three scleral regions (%).

Sample number	1	2	3	4	5	6	7	8	9	10 right	10 left	11	12	Mean	Median	SD
Age, sex	77MR	81FR	82FR	79ML	74FR	87ML	94FL	73ML	79MR	54F		38ML	81FL			
Pars Plana	34.99	32.54	30.28	29.3	26.98	23.46	24.88	37.93	26.99	29.48	25.03	23.59	58.51	31.07	29.3	9.34
3:00–3:30	27.85	22.67	27.26	19.18	25.18	21.89	19.66	28.68	31.47	28.89	23.97	19.53	43.07	26.1	25.18	6.47
5:00–5:30	24.24	17.65	19.55	13.48	19.77	19.5	19.44	16.64	24.23	26.72	20.27	23.09	50.95	22.73	19.77	9.18

M: male, R: right, F:female, L: left, SD: standard deviation.

substantially higher than the rest of their respective group distributions.

To assess the impact of these outliers, one-way ANOVA was performed both with and without their inclusion. The original analysis including outliers approached statistical significance (p=0.052), whereas the recalculated analysis excluding them revealed a significant difference among the groups (p<0.001). Post hoc testing with Bonferroni correction indicated a statistically significant difference in all three comparisons (pars plana versus 3:00–3:30: p=0.015; pars plana versus 5:00–5:30: p<0.001; 3:00–3:30 versus 5:00–5:30: p=0.022).

Comparison of reticular fiber density between the younger group (case 10: bilateral globes; case 1: unilateral) and the older group (10 globes) revealed no significant differences in any of the three regions (pars plana: p=0.362; 3:00–3:30: p=0.804; 5:00–5:30: p=0.108).

DISCUSSION

The present study characterized the distribution of reticular fibers in the human sclera, revealing substantial interindividual variability in fiber density. In most eyes, the highest density was observed in the anterior sclera, with a gradual decline toward the posterior region, and this trend was statistically supported. Notably, two eyes exhibited the lowest density, and one eye the highest density, in the mid-scleral region.

Reticular fibers contribute to the structural integrity of soft tissues by forming a cross-bridging framework with notable malleability [4]. A reduction in their density compromises this flexibility, rendering the tissue more vulnerable to deformation under mechanical stress [4]. In contrast, collagen fibers primarily confer tensile strength but lack comparable adaptability [4]; thus, in regions with diminished reticular fiber support, the sclera may be more prone to deformation in response to intraocular pressure.

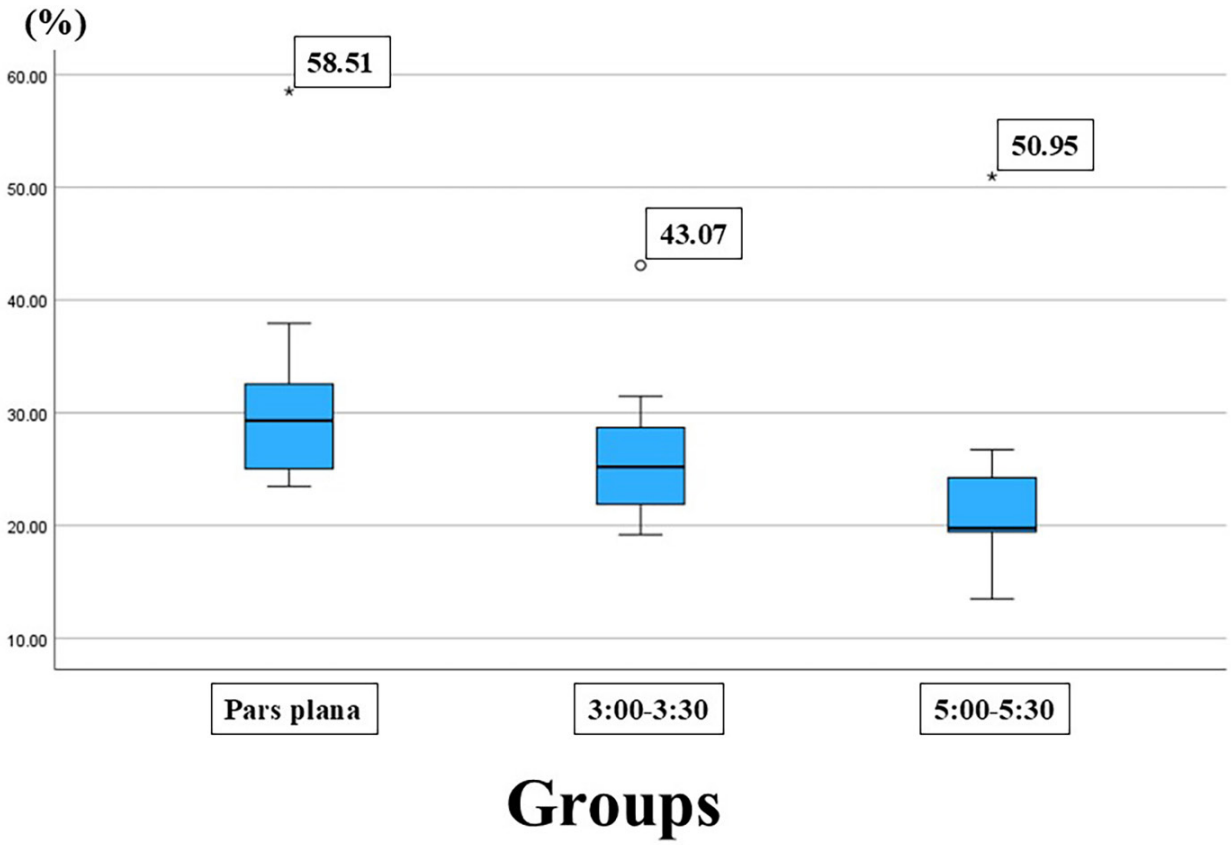

Figure 3. Three scleral regions are illustrated. Box-and-whisker plot of reticular fiber density across three scleral regions. Case 12 was identified as an outlier.

Reticular fiber density varied notably among individuals. The mean values and ranges were 31.07% (23.46%–58.51%) in the pars plana, 26.10% (19.18%–43.07%) at 3:00–3:30, and 22.70% (13.48%–50.95%) at 5:00–5:30. After excluding outliers, the recalculated averages were 28.19% (23.46%–37.93%) in the pars plana, 24.69% (19.18%–31.47%) at 3:00–3:30, and 20.38% (13.48%–26.72%) at 5:00–5:30. These findings suggest that reduced reticular fiber density might contribute to a predisposition toward pathologic myopia and posterior staphyloma in susceptible individuals.

In 10 of the 13 eyes, the highest density was observed in the anterior sclera, with a gradual decline toward the posterior

Figure 4. Overview of the sclera from a 77-year-old male. Scale bar means 1 mm. Circle indicates parts plana; dotted line, 3:00–3:30 region and square, 5:00–5:30 region.

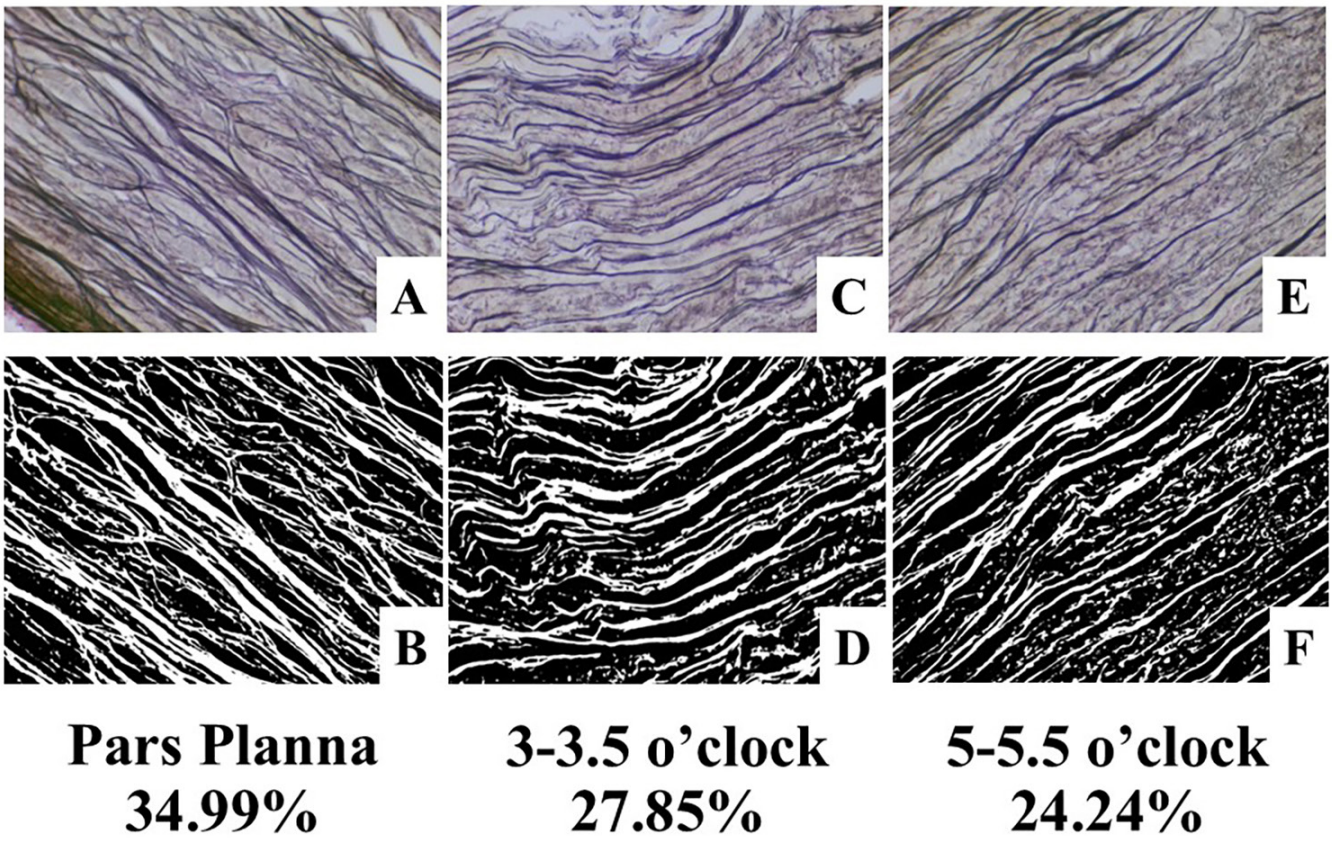

Figure 5. Reticular fiber density in the three regions from Figure 4, shows the highest density in the pars plana. Original magnification is x200. A and B demonstrate the pars plana with 34.99%., C and D, 3:00–3:30 with 27.85% and E and F, 5:00–5:30 with 24.24%.

regions. While scleral thickness generally increases posteriorly due to collagen accumulation [9], the observed decrease in reticular fiber density toward the posterior pole aligns with previous reports indicating that pathologic myopia tends to progress posteriorly [8], accompanied by localized scleral thinning [9].

Among the 13 eyes examined, 2 showed the lowest reticular fiber density at the 3:00–3:30 position, while 1 exhibited the highest density in the same region. These findings suggest that scleral weakness is not limited to the posterior pole. Such regional variability may help explain why posterior staphylomas can develop at different scleral sites [6]. In the two cases with the lowest density at 3:00–3:30—an 81-year-old female and a 38-year-old male—the sclera appeared thinner at this location (Figure 6 and Figure 7). The sample from the 81-year-old female showed no apparent anatomic abnormalities, likely reflecting natural thickness variation in one eye (Figure 6). The 38-year-old male specimen had a scleral laceration just beyond the 3:00 position; therefore, the image was captured at a stable point anterior to the lesion (figure not shown), which may have influenced the measurement. Conversely, the 79-year-old male sample with the highest density at 3:00–3:30 (Figure 8 and Figure 9) also showed no structural abnormalities, again suggesting individual variability in scleral thickness. Given that these three cases span a wide age range (38, 79, and 81 years), the observed differences do not appear to be age related. Although the underlying cause of such intraocular variability remains unclear, these findings imply that focal reductions in reticular fiber density outside the posterior pole may correspond to sites of localized scleral thinning.

Reticular fibers are known to undergo degenerative changes with aging [3]. Fragmentation and thickening are typical age-related alterations, resembling those observed in elastic fibers [3]. In addition to aging, other factors—such as elevated intraocular pressure—may also contribute to reticular fiber degeneration, potentially playing a role in the development of posterior staphyloma.

It is important to consider how alterations in reticular fibers may interact with collagen reorganization, fibroblast

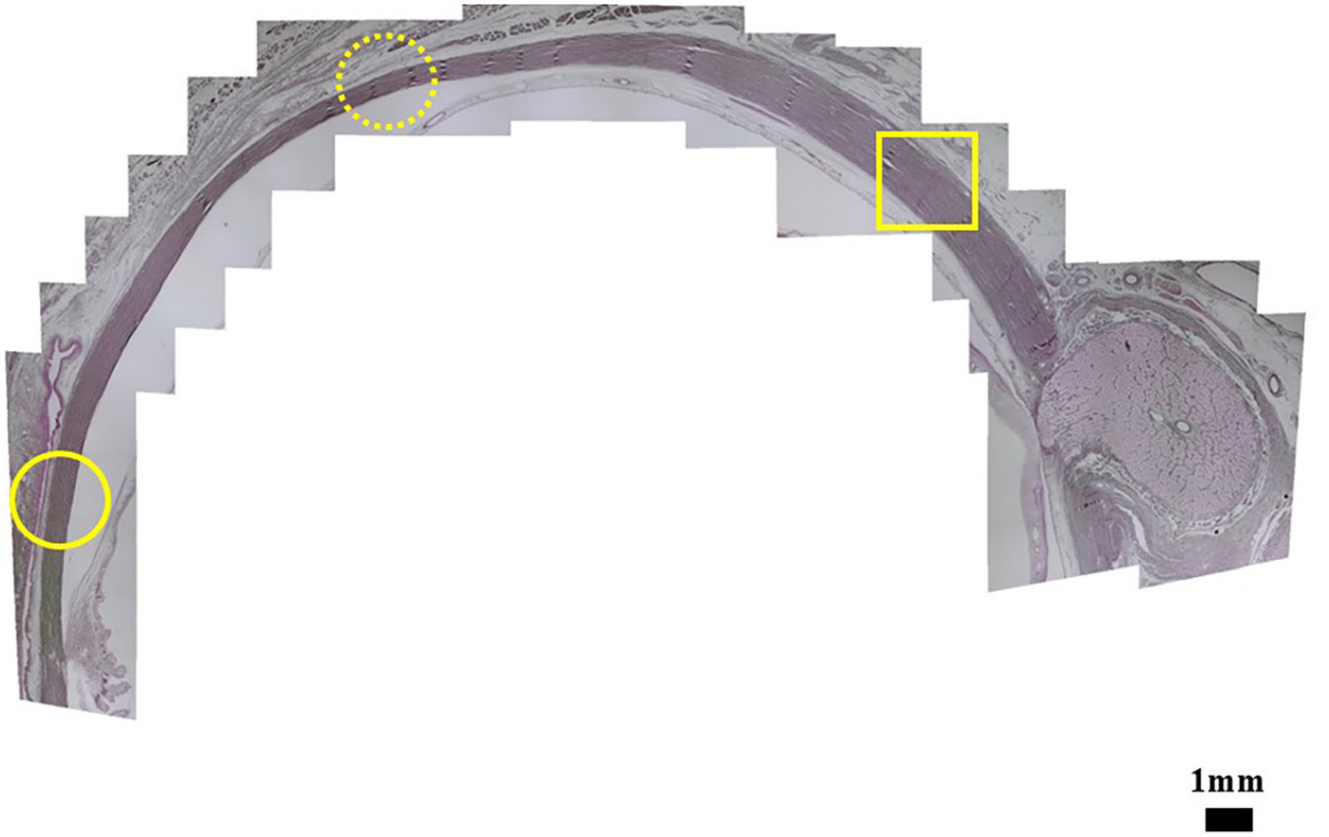

Figure 6. Overview of the sclera from an 81-year-old female. Scale bar means 1 mm. Circle indicates parts plana; dotted line, 3:00–3:30 region and square, 5:00–5:30 region.

activity, and extracellular matrix enzymes involved in scleral remodeling. While the presence of reticular fibers in the sclera has not been previously documented, type III collagen—the primary component of reticular fibers—has occasionally been reported in this tissue [14]. One proposed mechanism of myopia progression involves the negative remodeling of scleral collagen fibers under elevated intraocular pressure [15], leading to reduced fibroblast activity and matrix-degrading enzyme activity [16], as well as diminished synthesis of both type I and type III collagens [14]. Additionally, the cross-linking structures that stabilize collagen fibers are known to decline during this process [14]. Reticular fibers provide a supportive framework within connective tissues, while collagen fibers occupy the interstitial spaces to confer tensile strength [1]. Therefore, a reduction in type III collagen—corresponding to reticular fibers—alongside weakened cross-linking may significantly compromise the structural integrity of the sclera. Moreover, during myopia progression, fibroblasts actively secrete matrix metalloproteinases, which degrade extracellular matrix components, increase scleral compliance, and facilitate axial elongation [17].

Correlating histologic findings with clinical imaging is valuable for understanding scleral architecture in vivo. Optical coherence tomography studies of scleral thickness have largely been confined to the anterior segment, and even with swept-source optical coherence tomography, clear visualization of the posterior pole remains challenging. In contrast, a magnetic resonance imaging study assessing scleral thickness reported that in normal eyes, the equatorial region was the thinnest and the posterior pole the thickest [18]. However, in eyes predisposed to glaucoma, the posterior pole appeared thinner [18]. This observation aligns with the present study's finding that reticular fiber density tends to decrease toward the posterior pole, suggesting a possible structural basis for regional vulnerability.

From a clinical perspective, the findings of this study offer potential implications for both diagnosis and treatment. At present, reticular fiber density cannot serve as an

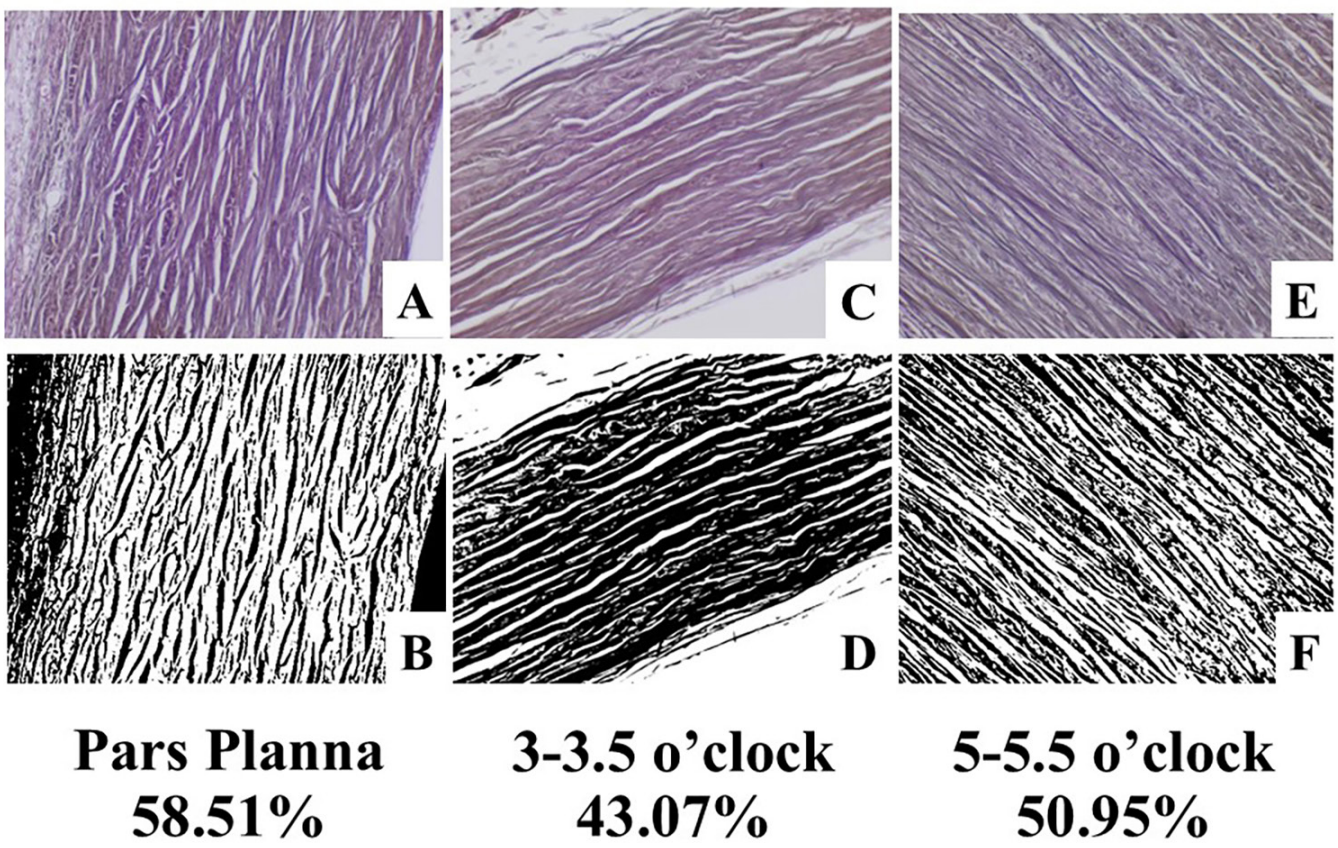

Figure 7. Reticular fiber density in the three regions from Figure 6, shows the lowest density at 3:00–3:30. Original magnification is x200. A and B demonstrate the pars plana with 58.51%., C and D, 3:00–3:30 with 43.07% and E and F, 5:00–5:30 with 50.95%.

early diagnostic marker for pathologic myopia or posterior staphyloma, as its assessment requires invasive scleral biopsy. However, if future imaging technologies enable noninvasive visualization of reticular fibers, their density may become a valuable biomarker for early detection. Regarding therapeutic approaches, red light therapy has been explored as a treatment for pathologic myopia [19,20]. Its proposed mechanism involves enhancing choroidal blood flow and increasing choroidal thickness [19,20]. Given its longer wavelength and deeper tissue penetration, red light may reach the sclera directly [21], potentially preserving reticular fiber integrity by reducing oxidative stress and suppressing inflammatory responses [22]. Interestingly, inflammation itself may contribute to the repair of damaged reticular fibers. During the early inflammatory phase of wound healing, reticular fibers transiently increase before being replaced by collagen fibers [12]. Understanding the mechanisms underlying this transient increase could provide novel therapeutic insights for managing pathologic myopia or posterior staphyloma after onset.

Although this study provides valuable insights into scleral thickness, regional variability, and their potential relationship to pathologic myopia, several limitations should be acknowledged. The relatively small sample size limits the generalizability of the findings. All cadavers were of East Asian descent, which may restrict applicability to other ethnic populations. Additionally, refractive error data were unavailable, preventing clear differentiation among normal eyes, highly myopic but nonpathologic eyes, and eyes with pathologic myopia. A control group of cadaveric eyes from individuals without a history of myopia was also lacking, making it difficult to determine whether the observed interindividual variability in reticular fiber density reflects disease-specific changes or normal physiologic variation. Future studies involving larger, more diverse populations and clinical correlation are necessary to validate and expand upon these results.

In conclusion, reticular fiber density in the sclera demonstrates substantial interindividual variability. Notably, regions of scleral structural vulnerability are not confined

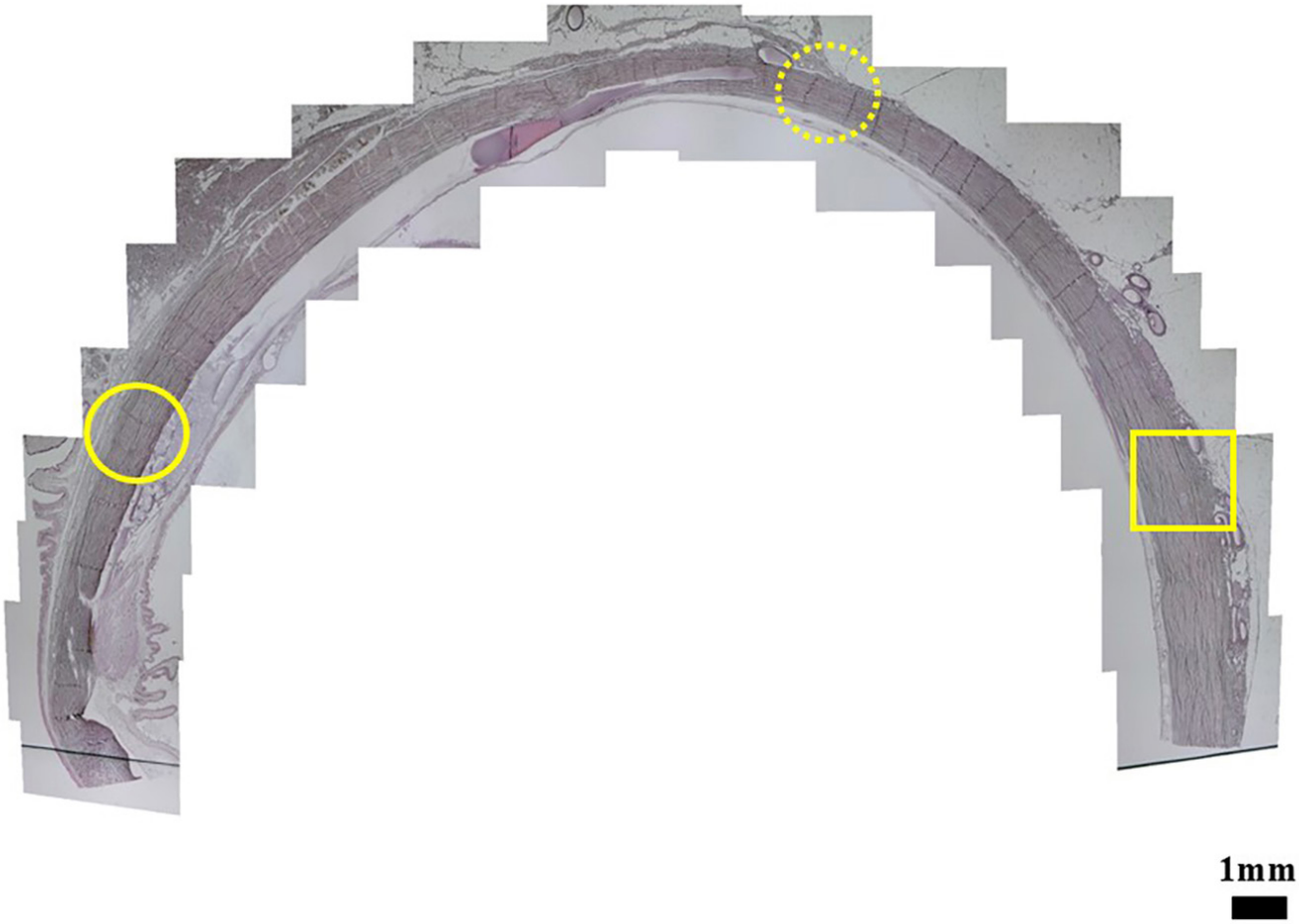

Figure 8. Overview of the sclera from a 79-year-old male. Scale bar means 1 mm. Circle indicates parts plana; dotted line, 3:00–3:30 region and square, 5:00–5:30 region.

to the posterior pole, which may help explain the diverse anatomic distribution of posterior staphylomas. Given the critical role of the reticular fiber framework in maintaining scleral integrity, reduced fiber density may be associated with a predisposition to pathologic myopia and the development of posterior staphylomas. However, further investigation is needed to clarify the nature and extent of this association.

ACKNOWLEDGMENTS

We gratefully acknowledge Professor Gangadhara Sunder of the Orbit & Oculofacial Surgery Service, Department of Ophthalmology, National University Hospital, Singapore, for his valuable contributions to this research. Funding: The authors declare that no funds, grants, or other support were received during the preparation of this manuscript. Competing interests: The authors report no financial or non-financial interests to disclose. Ethical approval: The institutional review board (IRB) of Dong-A University Hospital approved this study (approval number: DAUHIRB-EXP-25–114), which was conducted in accordance with the tenets of the Declaration of Helsinki and its later. Consent to participate: Informed consent was waived by the IRB due to this being an anatomic and non-interventional study. All authors have read and approved the final version of the manuscript. No individuals who do not meet the authorship criteria have been included as authors.

REFERENCES

1. Ushiki T. Collagen fibers, reticular fibers and elastic fibers. A comprehensive understanding from a morphological viewpoint. Arch Histol Cytol 2002; 65:109-26. [PMID: 12164335].

2. Chapter 4: Connective Tissue. In Gartner LP & Hiatt JL, eds. Color Atlas and Text of Histology. 7th ed. Philadelphia: Wolters Kluwer; 2017. p. 61–84.

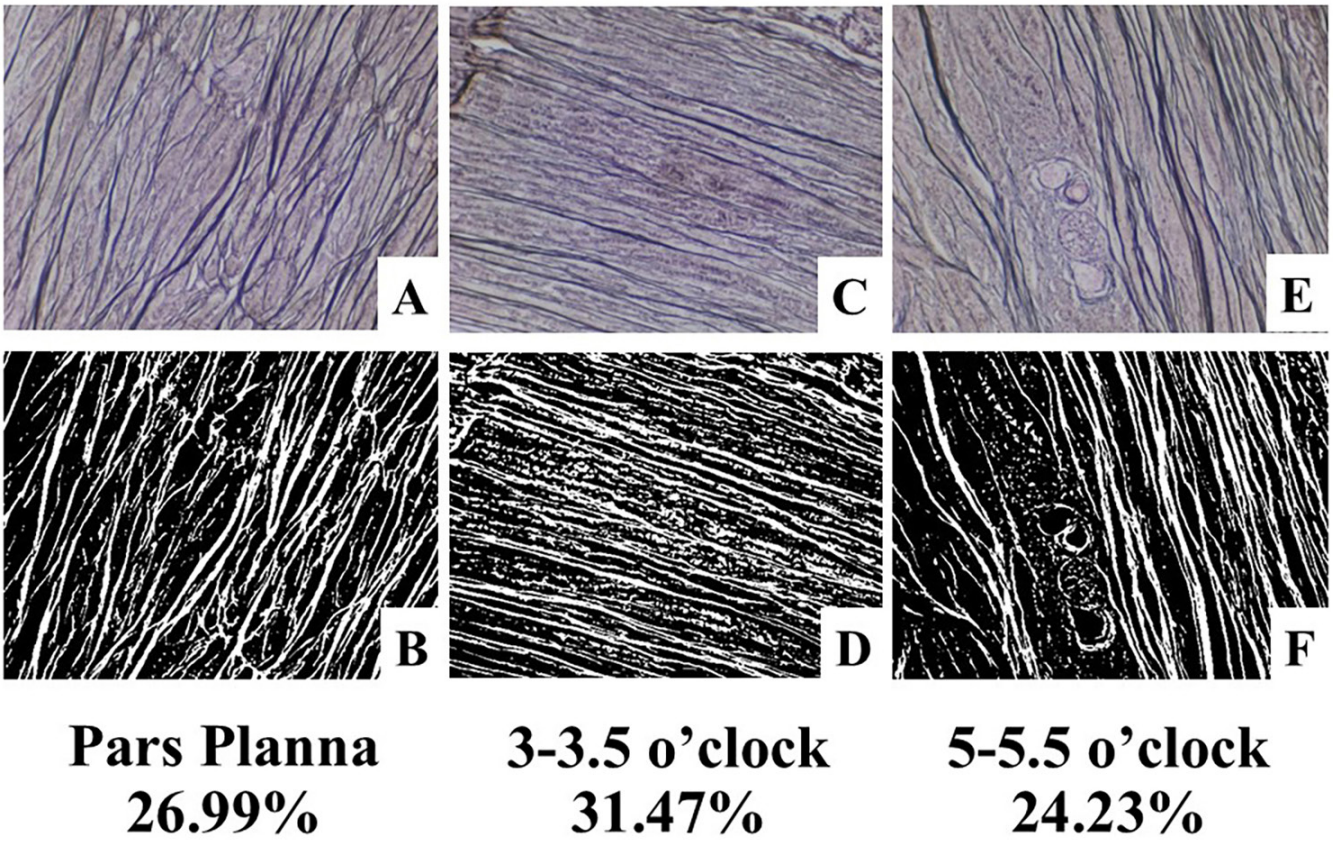

Figure 9. Reticular fiber density in the three regions from Figure 8, shows the highest density at 3:00–3:30. Original magnification is x200. A and B demonstrate the pars plana with 26.99%., C and D, 3:00–3:30 with 31.47% and E and F, 5:00–5:30 with 24.23%.

3. Kakizaki H, Ali MJ. Age-related changes in the reticulin fibers of the lacrimal sac. Saudi J Ophthalmol 2025; 39:243-5. [PMID: 41179381].

4. Tanaka T. What is the fibers stained by the silver stainig? Kensatogijutsu 1996; 24:753-7. Japanese.

5. Moriyama M, Ohno-Matsui K, Hayashi K, Shimada N, Yoshida T, Tokoro T, Morita I. Topographic analyses of shape of eyes with pathologic myopia by high-resolution three-dimensional magnetic resonance imaging. Ophthalmology 2011; 118:1626-37. [PMID: 21529960].

6. Ohno-Matsui K. Proposed classification of posterior staphylomas based on analyses of eye shape by three-dimensional magnetic resonance imaging and wide-field fundus imaging. Ophthalmology 2014; 121:1798-809. [PMID: 24813630].

7. Curtin BJ. The posterior staphyloma of pathologic myopia. Trans Am Ophthalmol Soc 1977; 75:67-86. [PMID: 613534].

8. Jonas JB, Xu L. Histological changes of high axial myopia. Eye (Lond) 2014; 28:113-7. [PMID: 24113300].

9. Vurgese S, Panda-Jonas S, Jonas JB. Scleral thickness in human eyes. PLoS One 2012; 7:e29692[PMID: 22238635].

10. Jonas JB, Wang YX, Dong L, Guo Y, Panda-Jonas S. Advances in myopia research anatomical findings in highly myopic eyes. Eye Vis (Lond) 2020; 7:45-[PMID: 32905133].

11. Grytz R, Yang H, Hua Y, Samuels BC, Sigal IA. Connective Tissue Remodeling in Myopia and its Potential Role in Increasing Risk of Glaucoma. Curr Opin Biomed Eng 2020; 15:40-50. [PMID: 32211567].

12. Singh D, Rai V, Agrawal DK. Regulation of Collagen I and Collagen III in Tissue Injury and Regeneration. Cardiol Cardiovasc Med 2023; 7:5-16. [PMID: 36776717].

13. Grizzle WE. Theory and practice of silver staining in histopathology. J Histotechnol 1996; 19:183-95. .

14. Sun Y, Sha Y, Yang J, Fu H, Hou X, Li Z, Xie Y, Wang G. Collagen is crucial target protein for scleral remodeling and biomechanical change in myopia progression and control. Heliyon 2024; 10:e35313[PMID: 39170348].

15. Wang P, Kong K, Jiang J, Jiang J, Xie Z, Lin F, Song Y, Fang X, Jin L, Li F, Wang W, Du S, Shi Z, Zeng J, Zhang X, Chen S. Glaucoma Suspects with High Myopia Study Group. Intraocular pressure is a promising target for myopia control. J Transl Med 2025; 23:556-[PMID: 40380302].

16. Yin X, Ge J. The Role of Scleral Changes in the Progression of Myopia: A Review and Future Directions. Clin Ophthalmol 2025; 19:1699-707. [PMID: 40433505].

17. Xiao K, Chen Z, He S, Long Q, Chen Y. The role of NF-κB pathway and its regulation of inflammatory cytokines in scleral remodeling of form-deprivation mice model. Immunol Res 2025; 73:48-[PMID: 39920470].

18. Norman RE, Flanagan JG, Rausch SMK, Sigal IA, Tertinegg I, Eilaghi A, Portnoy S, Sled JG, Ethier CR. Dimensions of the human sclera: Thickness measurement and regional changes with axial length. Exp Eye Res 2010; 90:277-84. [PMID: 19900442].

19. Zheng Z, Jiang X, Chen R, Dong L. Efficacy comparison of atropine, orthokeratology and repeated low-level red-light therapy for myopia control in children: a systematic review and network meta-analysis. Br J Ophthalmol 2025; 109:1215-20. [PMID: 40610049].

20. Zhang G, Jiang J, Qu C. Myopia prevention and control in children: a systematic review and network meta-analysis. Eye (Lond) 2023; 37:3461-9. [PMID: 37106147].

21. Zein R, Selting W, Hamblin MR. Review of light parameters and photobiomodulation efficacy: dive into complexity. J Biomed Opt 2018; 23:1-17. [PMID: 30550048].

22. Hamblin MR. Mechanisms and applications of the anti-inflammatory effects of photobiomodulation. AIMS Biophys 2017; 4:337-61. [PMID: 28748217].